

1 **Supporting Information for**

2 **Local Mixing Governs the Buildup of Humid Heat Events in the World's Leading Hotspot**

3 **Qin Jiang, Steven C. Sherwood, Martin S. Singh, and Paul A. O’Gorman**

4 **Corresponding Author: Qin Jiang**

5 **drqinjiang@gmail.com**

6 **This PDF file includes:**

7 Supporting text

8 Figs. S1 to S8

9 SI References

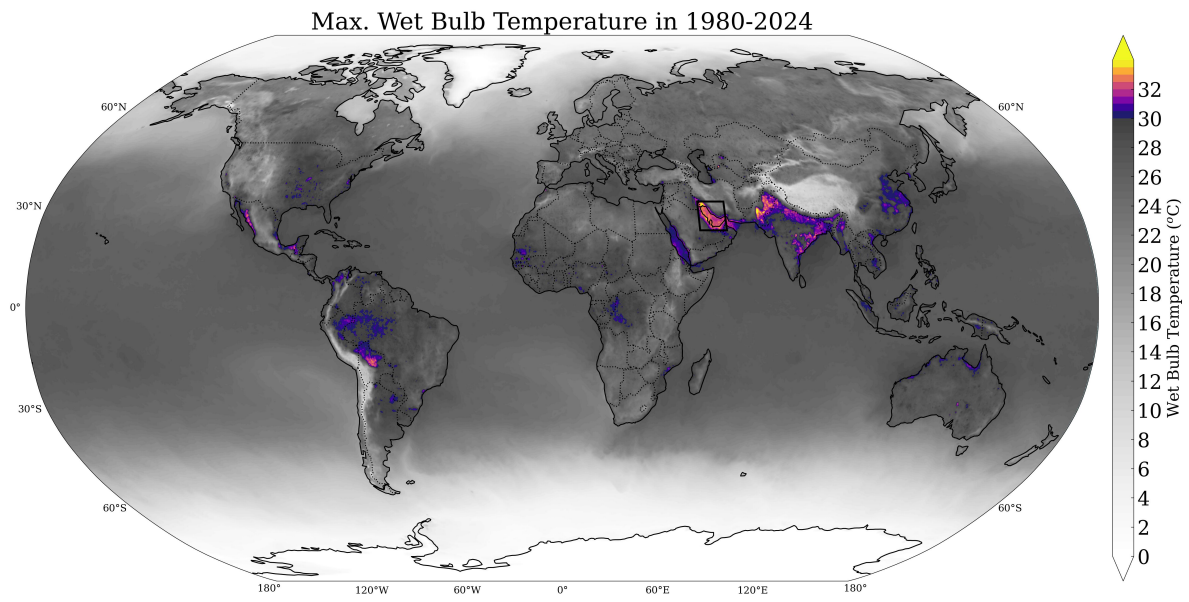


Fig. S1. Global distribution of local all-time maximum wet-bulb temperature (T_w ; °C) in 1980-2024 based on ERA5 reanalysis.

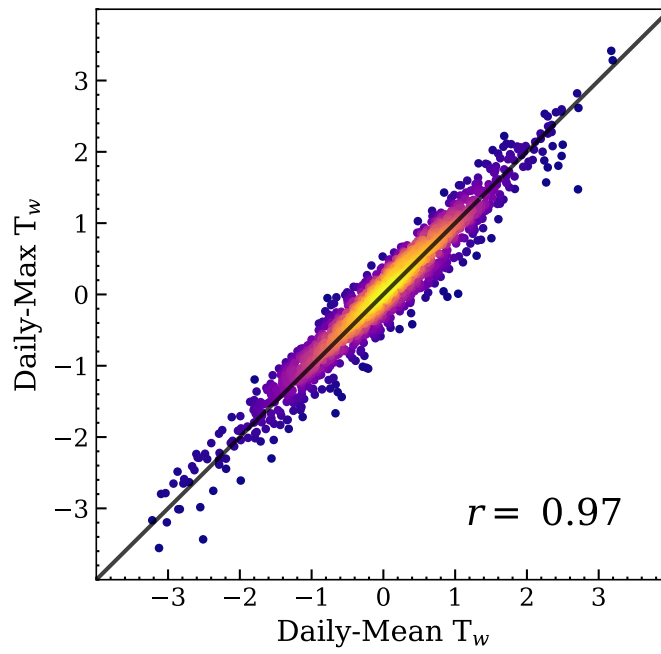


Fig. S2. As in Fig. 2 in the main manuscript, but for correlation between anomalies of daily mean T_w and daily maximum T_w .

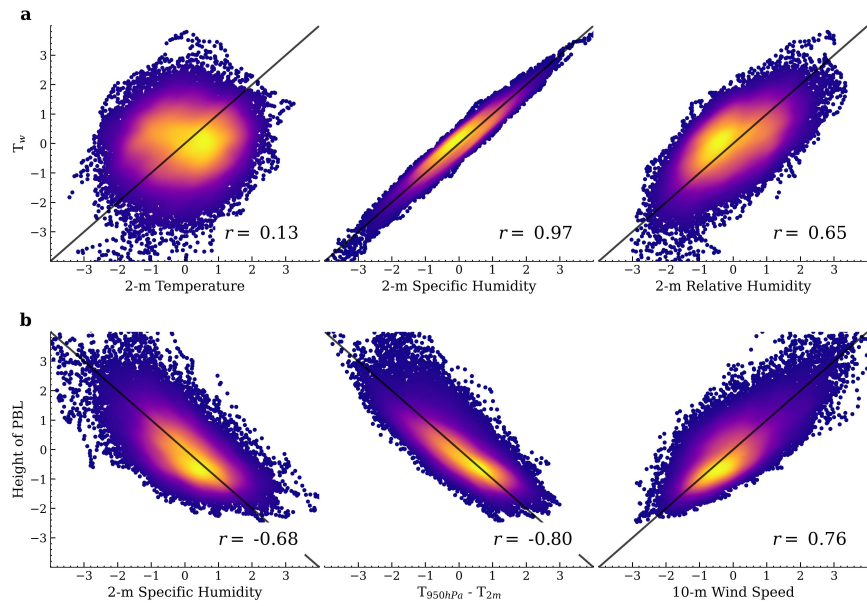


Fig. S3. As Fig. 2 in the main manuscript, but for hourly data.

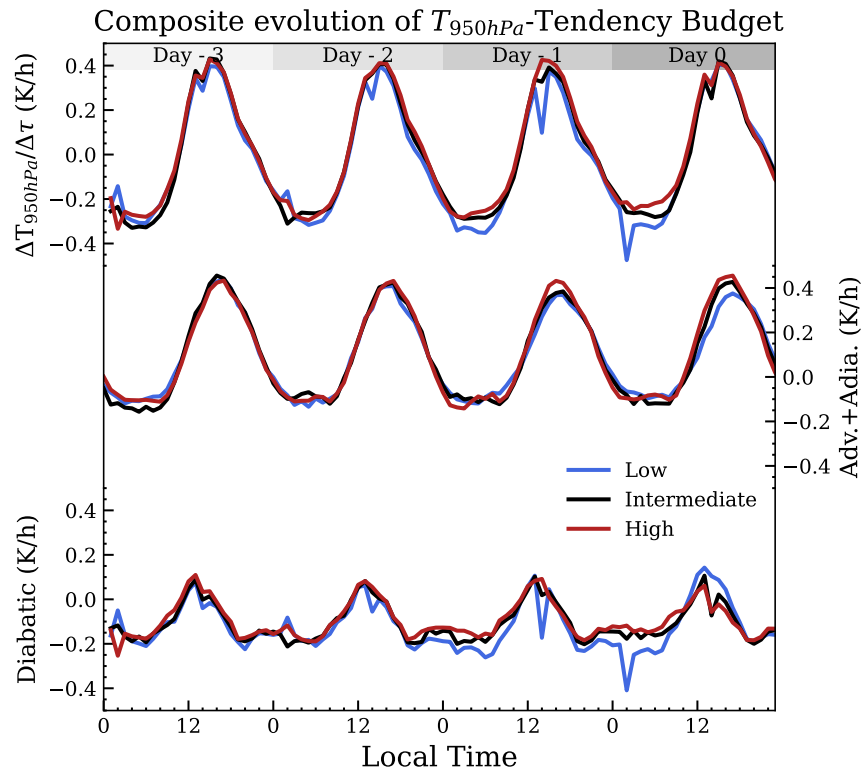


Fig. S4. Hourly composite timeseries of $T_{950\text{hPa}}$ -tendency budget for high-, intermediate-, and low- T_w days. Subpanels show the total $T_{950\text{hPa}}$ tendency (top), tendency driven by three-dimensional advection and adiabatic heating in subsidence (middle), and the diabatic contribution (bottom; calculated as the residual of the first two terms). Each term is calculated in Eulerian coordinates and spatially averaged over the Gulf. Focusing on their magnitudes, the buildup of the capping inversion (positive part of $\Delta T_{950\text{hPa}}/\Delta\tau$) is mainly governed by advection and adiabatic heating, with some compensation coming from diabatic processes.

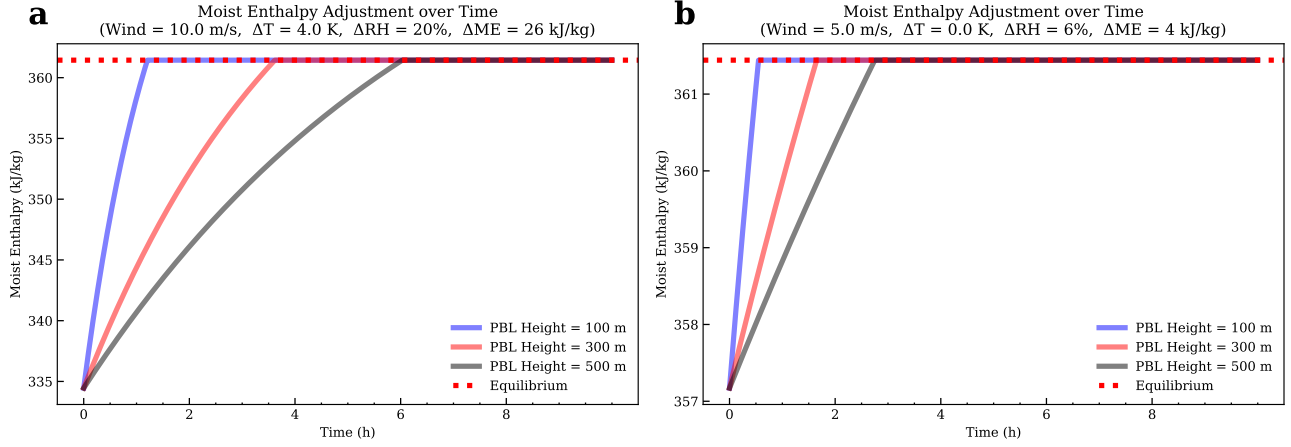


Fig. S5. Numerical integrated time series of moist enthalpy (ME) for two conditions based on Equations. (1-2); see Supporting Information Text below. Three solid lines denote experiments with different PBL height, and the dashed line denotes the pre-specified equilibrium state. ΔT , ΔRH , and ΔME denote the deficits of temperature, relative humidity, and ME at 2 m AGL. required to reach the equilibrium state

10 Supporting Information Text

11 **Equilibrium Adjustment Timescale.** The simplified numerical solution of the ME adjustment is based on:

$$12 \quad \rho h \frac{dME}{dt} = F \quad [1]$$

$$13 \quad F = \rho C_T v_{sfc} (ME_{sfc} - ME_{2m}) \quad [2]$$

14 where F contains both sensible and latent heat flux. h is the PBL height. v_{sfc} is the surface wind speed. C_T is the
15 nondimensional aerodynamic flux coefficient, equal to 0.002. ρ is the density.

16 By reorganizing the equation and integrating from $t = 0$ to time t :

$$17 \quad \int_{ME_{initial}}^{ME_{2m}} \frac{dME_{2m}}{ME_{sfc} - ME_{2m}} = \int_0^t \frac{1}{\tau} dt \quad [3]$$

18 where $\tau = \frac{h}{C_T v_{sfc}}$, and it yields:

$$19 \quad ME_{2m}(t) = ME_{sfc} - (ME_{sfc} - ME_{initial}) e^{-t/\tau} \quad [4]$$

$$20 \quad t = -\tau \ln \left(\frac{ME_{sfc} - ME_{2m}(t)}{ME_{sfc} - ME_{initial}} \right) \quad [5]$$

21 Therefore, given a value of $ME_{2m}(t)$, we can obtain an analytical solution for the adjustment timescale t . Mathematically, t
22 goes to infinity as the system approaches a strict equilibrium, $ME_{sfc} - ME_{2m} = 0$. However, because realistic surface fluxes
23 do not vanish even in a steady state (i.e., a consistent diurnal evolution of ME over several days), the sustained flux indicates a
24 potential equilibrium maximum of ME.

25 Considering an e -folding timescale, it gives:

$$26 \quad t = \frac{h}{C_T v_{sfc}} \quad [6]$$

27 which assumes an equilibrium maximum at $\frac{ME_{sfc} - ME_{2m}(t)}{ME_{sfc} - ME_{initial}} = \frac{1}{e}$; therefore, as an example, $t \approx 13.9h$ with 500 m of h and 5
28 m/s of v_{sfc} . Alternatively, in the Fig. S5, we apply a common value of observed ΔT (relative to the surface) and RH during a
29 humid heat extreme as an equilibrium maximum. We specify the ME_{sfc} as $T_{sfc} = 305K$ with 100% evaporation availability, and
30 assume an equilibrium maximum of ME with a temperature 1K below T_{sfc} with 80% RH. The initial state is hence described
31 by the ΔT , ΔRH , and ΔME required to reach equilibrium, listed as the sub-titles.

32 This simplified framework assumes that the ME builds up exclusively via surface flux, neglecting other ME sources and
33 dissipation processes. The PBL is assumed to be well-mixed with the same specific humidity as the 2-m layer. Shallower PBL
34 adjusts ME faster. The timescale to reach equilibrium varies with conditions, but all of them are on the order of a few hours,
35 which is faster compared to the multi-day buildup of observed humid heat events. The ΔME in Fig. S5a represents an extreme
36 scenario, exceeding the typical energy required to build a general humid heat event [i.e., composite $\Delta ME = \Delta MSE < 20$

37 kJ/kg (1, 2)]. The ΔME in Fig. S5b is close to the ME deficit between **Consistent** and **Control** discussed in the main text.
38 Considering ME dissipation processes, the timescale are expected to larger than those shown in Fig. S5, but potentially
39 within Equation 6. Nevertheless, all experiments take a few hours to reach the pre-specified equilibrium maximum, supporting
40 the idea that the PBL condition associated with humid heat events shall have sufficient time to equilibrate. Without changes
41 in equilibrium maximum and input sources, the daily maximum T_w is capped by the equilibrium threshold, while PBL height
42 only affects the timescale to reach that threshold in the budget framework. Our study will further show that suppressed local
43 mixing associated with shallower PBL height can break through this equilibrium threshold.

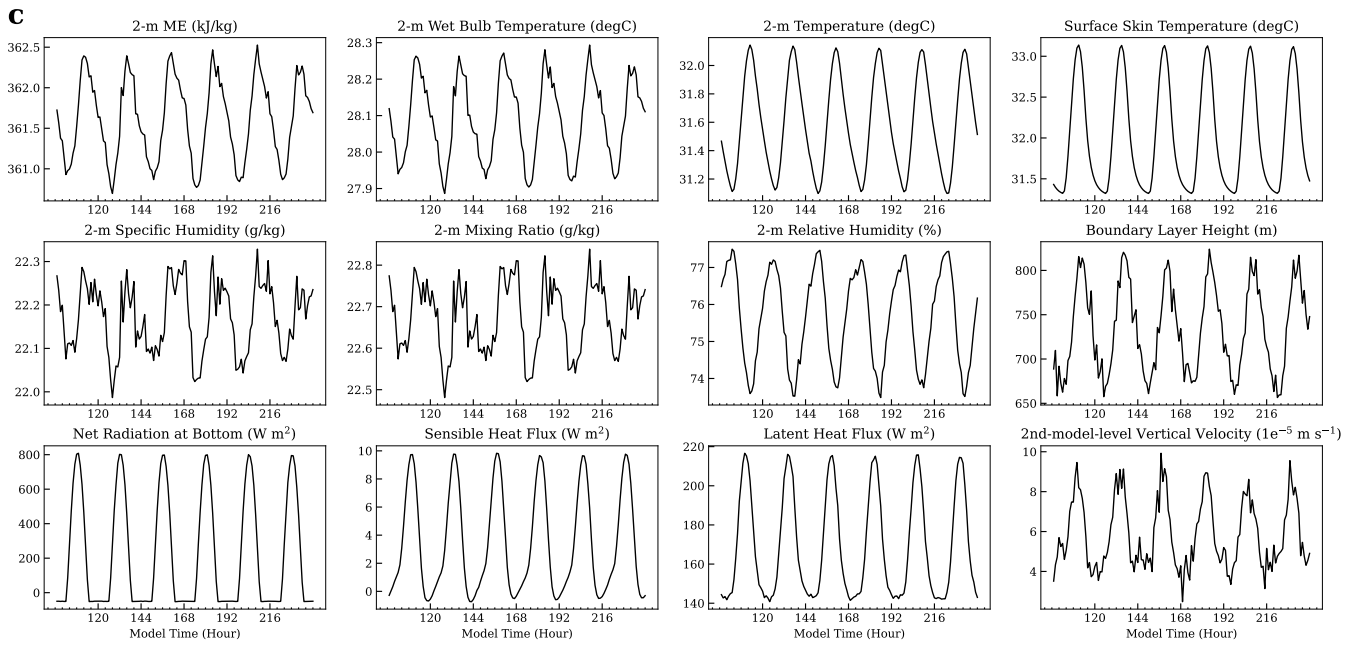
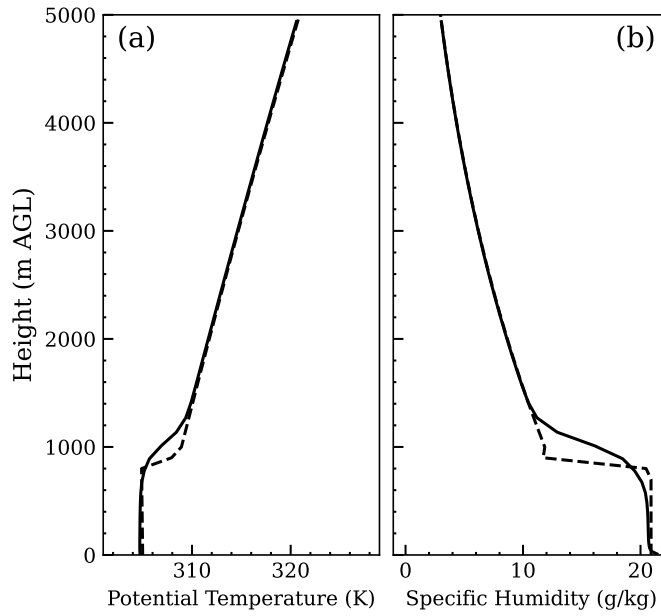


Fig. S6. (a-b) Vertical profile of potential temperature and specific humidity of input sounding (dashed lines) and domain-averaged, daily-mean sounding during 4-10th days in **Control** LES simulation (solid line). (c) Diurnal cycle of the domain-averaged fields in the control simulation. The results show a steady diurnal evolution of a well-mixed PBL achieved by the current LES model setup.

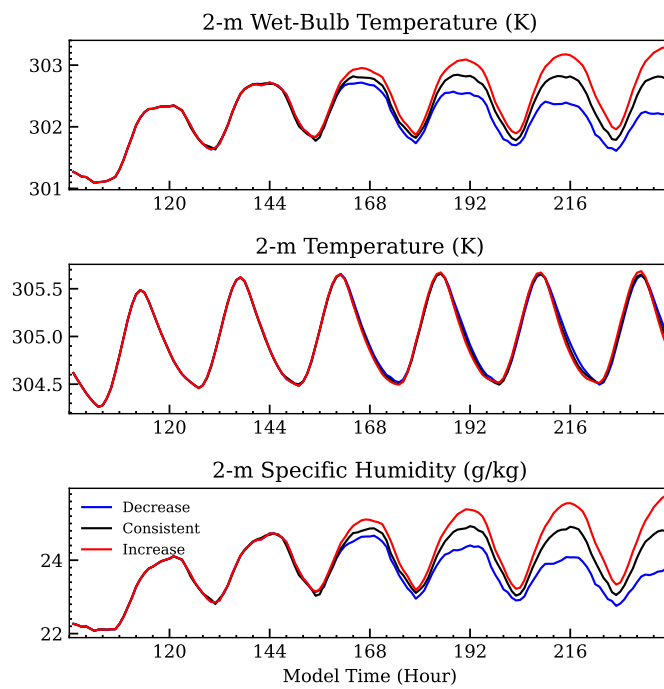


Fig. S7. Time series of LES-simulated T_w , temperature, and specific humidity at 2 m AGL for **Decrease**, **Consistent**, and **Increase** experiments, respectively, which roughly reproduce the behaviors shown in Fig. 3d in the main manuscript.

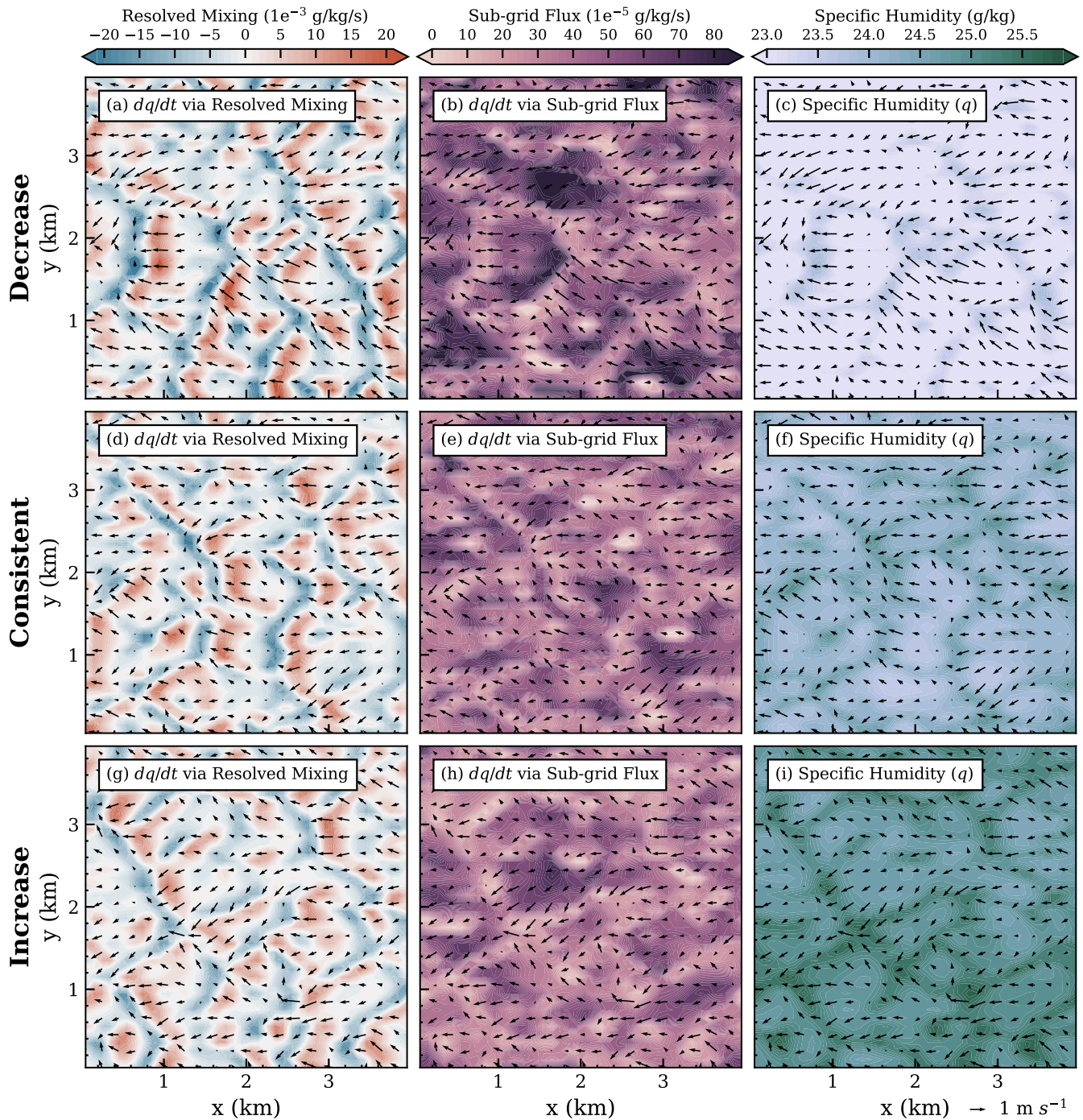


Fig. S8. Plan view of specific humidity (q) tendency via resolved mixing and sub-grid flux, and specific humidity, q , at 8 pm on the final day of simulations for **Decrease**, **Consistent**, and **Increase** experiment, respectively. The budget is calculated at the second model level, around 30 m AGL.

44 **References**

- 45 1. Y Zhang, WR Boos, An upper bound for extreme temperatures over midlatitude land. *Proc. Natl. Acad. Sci.* **120** (2023).
46 2. F Li, T Tamarin-Brodsky, Atmospheric stability sets maximum moist heat and convection in the midlatitudes. *Sci. Adv.*
47 **12** (2026).